Scientific Papers. Series E. Land Reclamation, Earth Observation & Surveying, Environmental Engineering. Vol. XV, 2026
Print ISSN 2285-6064, CD-ROM ISSN 2285-6072, Online ISSN 2393-5138, ISSN-L 2285-6064

# SEISMIC SURVEY FOR SHALLOW INVESTIGATION OF $CO_2$ MIGRATION PATHWAYS IN BĂILE LĂZĂREȘTI, ROMANIA

**Marius-Bogdan BĂRĂITĂREANU[1, 2], Ionelia PANEA[2], Alexandra Constanța DUDU[1], Andrei Gabriel DRAGOȘ [1, 3], Gabriel IORDCHE[1], Lia STELEA[1, 3], Sorin ANGHEL[1]**

[1]National Research and Development Institute for Marine Geology and Geoecology, GeoEcoMar, 23-25 Dimitrie Onciul Street, 024053, District 2, Bucharest, Romania
[2]Faculty of Geology and Geophysics, University of Bucharest, 1 Nicolae Bălcescu Blvd, 010041, District 1, Bucharest, Romania
[3]Doctoral School of Geology, Faculty of Geology and Geophysics, University of Bucharest, 1 Nicolae Bălcescu Blvd, 010041, District 1, Bucharest, Romania

Corresponding author email: bogdan.baraitareanu@geoecomar.ro

***Abstract***

*At the Lăzărești mofette site in Transylvania, Romania, carbon dioxide migrates upward from depth along fault systems, reaching the shallow subsurface where these pathways branch into faults and fissures. To identify these structures, active-source seismic reflection measurements were performed along a linear profile. Seismic energy was generated using a 10-kg sledgehammer at shot points spaced 1 m apart. Forty SmartSolo vertical-component (5 Hz) receivers were deployed at 1 m spacing along a seismic profile located near two natural carbonated water springs, with the aim of imaging the subsurface pathways that enable carbonated water to reach the surface. After data processing, high-amplitude reflections were identified, corresponding to $CO_2$-bearing, water-saturated formations. Understanding the natural mechanisms of $CO_2$ migration to the surface provides a valuable natural analogue for assessing the safety and long-term behavior of geological $CO_2$ storage associated with major industrial emitters, such as thermal power plants or cement factories.*

***Key words****: carbon dioxide, faults, mofettes, reflection, seismics.*

## INTRODUCTION

Natural systems where $CO_2$ is emitted to the surface, such as areas with mofettes and carbonated springs, represent natural laboratories in which the migration pathways of gases originating from depth can be observed and analysed (Pearce et al., 2004). Studying these environments provides important insights into the mechanisms that control the ascent of $CO_2$ through fault and fracture networks toward the surface (Annunziatellis et al., 2008). Such observations are particularly relevant in the context of $CO_2$ geological storage, where understanding potential migration pathways, leakage mechanisms and possible environmental impacts are essential to increase storage safety and support public trust in the technology (Metz et al., 2005). Identification of migration pathways for $CO_2$ geological storage and also for studying the leakage mechanisms from the natural laboratories can be supported by the active-source seismic method. This method is a versatile tool employed across a broad spectrum of projects, including geotechnical evaluations for civil engineering and hydrogeological studies (Pelton, 2005). This approach is applicable to both near-surface studies and deep-crustal investigations reaching several kilometres, supporting both 2D and 3D data volumes (Cox et al., 2020). The principle of the method is to generate controlled seismic waves that travel through the Earth, reflect at boundaries between different geological layers, and are recorded at the surface by strategically arranged sensors (Cîndea, 1965; Sheriff & Geldart, 1995). The technique is especially effective for mapping layer geometry, faults, fractures and variations in lithology and fluid content (Telford et al., 1990), with results interpreted through advanced data-processing workflows (Yilmaz, 2001; Panea, 2019). In the context of $CO_2$ storage, this method is particularly valuable for characterizing potential

reservoirs and cap rocks, identifying structural traps or leakage pathways, and monitoring changes in the subsurface caused by $CO_2$ injection, thereby supporting safe site selection and long-term storage integrity. Therefore, the seismic method was used to identify migration pathways of $CO_2$ from depth to the surface in a natural laboratory from Romania for the study of $CO_2$ leakage mechanisms that could be associated with an anthropogenic storage.

## MATERIALS AND METHODS

Băile Lăzărești site, Harghita county, is recognized for its dry and wet mofettes with high $CO_2$ concentrations (Dudu et al., 2024). Several surveys were deployed over the years, starting in 2019, to assess the $CO_2$ fluxes, the geological structure and the $CO_2$ migration mechanisms. In order to identify the shallow geological structure, especially fractures in the uppermost tens of meters, a seismic profile was made in April 2025. The profile, marked with blue line on the map from Figure 1, was placed next to $CO_2$ water springs (marked with red circles on the map).




Figure 1. Map of the Băile Lăzărești perimeter showing the geophone profile and the natural $CO_2$-rich water springs

The profile consisted of 40 single-channel SmartSolo geophones with a 5Hz frequency, positioned on a line intersecting potential fractures, faults, or stratigraphic boundaries that might act as primary conduits for carbon dioxide moving upward to the surface. A 1 m spacing was maintained between these sensors, and generation points were similarly established at 1 m intervals, located directly at each geophone station. The waves were generated using a 10 kg hammer that struck a metal plate (Figure 2). To ensure high spatial accuracy, the coordinates and elevations for every geophone and each generation point were registered using a Trimble R980 GNSS system.



Figure 2. Generation of the seismic waves

After data acquisition, the recorded information was retrieved and prepared for subsequent analysis. The analysis was made with SoloLite program. The continuous seismic data gathered over several hours on-site were partitioned so that every hammer strike was isolated into a two-millisecond window. The exact moment of each impact was determined using the data provided by the sensor attached to the hammer during the acquisition phase (Figure 3).



Figure 3. Hammer and the sensor attached on it

The timing for every hammer hit was logged in the SoloTB mobile application and exported as an .sso file, which was then imported into the SoloLite software to isolate only the time segments required for data refinement. Additionally, the software allows for the validation of sensor coordinates, making it possible to confirm the precise location and elevation of each deployed unit.

## RESULTS AND DISCUSSIONS

Within this study, we performed an analysis of the relative energy distribution along the entire length of the seismic profile, based on the signal variations generated by hammer impact. This analysis produces a two-dimensional relative energy map, where a colour gradient serves as a visual indicator: blue tones represent low energy values, whereas yellow and red hues highlight regions of high intensity (Figure 4). This mapping is instrumental for enhancing data visualization and interpretation, as it enables direct correlation with seismic sections in both the time and depth domains.

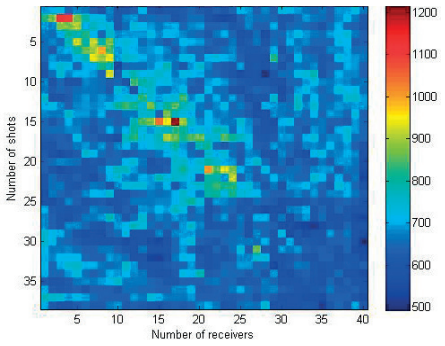



Figure 4. 2D map for relative energy distribution along the seismic line

Figure 4 highlights a non-uniform distribution of relative energy along the seismic line. The highest energy values are recorded in the initial segment of the receiver spread, extending from the first geophone up to approximately geophone 30. In this interval, the signal amplitudes are noticeably stronger, corresponding to the lighter colour tones on the map. Beyond this point, toward the distal end of the profile, a gradual reduction in recorded energy is evident, reflected by the predominance of darker blue shades.

To eliminate the influence of surface relief on reflection travel times, elevation (static) corrections were computed and applied to the seismic dataset. A horizontal reference datum positioned at +750 m - corresponding to the highest elevation along the profile - was selected as the correction level. This choice ensured that topographic variations along the line were properly accounted for without introducing excessive static shifts. Selecting a reference datum substantially above the maximum elevation of the profile would have generated significantly larger static correction values. On the other hand, defining the datum below the ground surface would result in the removal of shallow structural information located between the actual surface and the reference level. The variation in topography along the seismic profile is presented in Figure 5 while the corresponding elevation corrections, computed relative to the +750 m reference datum, are presented in Figure 6.

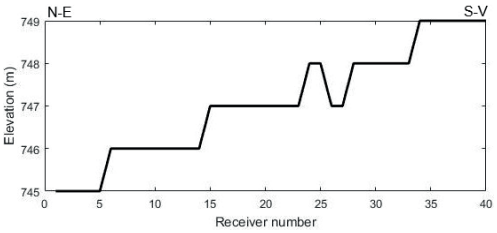



Figure 5. Topographic relief variation along the seismic line

As shown in the topographic profile of the seismic line, elevation increases progressively from geophone 1 to geophone 40, with an approximate elevation difference of 4 m between these points.

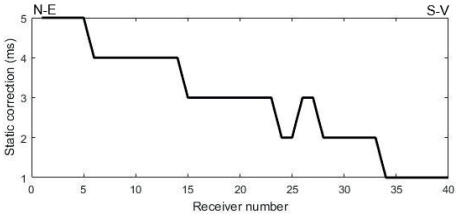



Figure 6. Static corrections for the +750 datum

In shallow seismic reflection processing, band-pass filtering represents a fundamental operation aimed at enhancing data quality and facilitating the interpretation of subsurface reflectors. This procedure is based on the principle that coherent reflection energy is typically concentrated within a limited frequency interval, whereas a significant portion of the unwanted noise occupies frequencies outside this band. By retaining the spectral components associated with reflection events and attenuating those linked to noise, frequency filtering increases the clarity of coherent arrivals and improves the overall signal-to-noise ratio. The design of the filter is guided by spectral analysis, which allows identification of the dominant frequency content of both signal and noise. In near-surface investigations, the effective pass-band generally extends toward higher frequencies compared to deep seismic surveys, reflecting the shorter travel times and the higher-frequency content of hammer-generated sources. However, the selected bandwidth must remain sufficiently broad to preserve wavelet shape and maintain vertical resolution. Figure 7 presents an example of an unprocessed common-source gather (CSG).

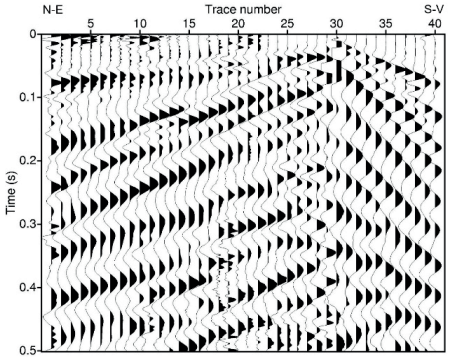



Figure 7. Common-source gather; shot-point location at x = 30 m

The record includes high-amplitude surface waves that require attenuation, together with reflection events that must be preserved during filtering. The choice of cut-off frequencies was determined following examination of the seismic data in the f–k domain, where the distribution of energy in frequency–wavenumber space can be evaluated. The corresponding f–k amplitude spectrum (Figure 8) indicates that surface waves dominate frequencies up to approximately 60 Hz, whereas reflection energy exhibits significant amplitudes primarily within the 35-40 Hz range.

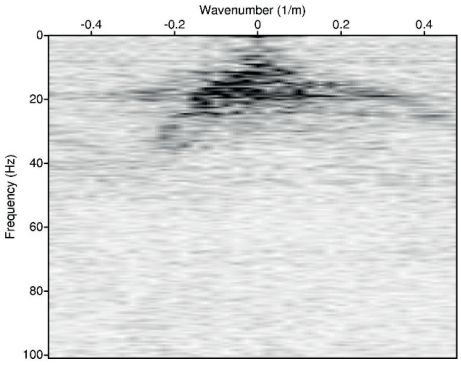



Figure 8. f-k amplitude spectrum of common-source gather from Figure 7

Applying a band-pass filter that overlaps the frequency interval shared by both surface waves and reflected arrivals results in the retention of both energy types within the dataset. For instance, the common-source gather illustrated in Figure 7 was processed using a 10-30 Hz band-pass filter. Within this frequency window, a substantial portion of the surface-wave energy remains visible alongside the reflection signal. When the filter band-pass is shifted toward higher frequencies, surface-wave energy is attenuated more effectively, while reflection events become comparatively more pronounced. This effect is evident in Figure 9, where a 26-50 Hz band-pass filter was applied.

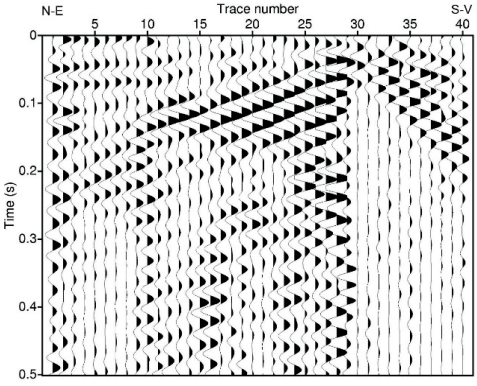



Figure 9. Common-source gather after band-pass frequency filtering applied for 26-50 Hz; shot point location at x = 30 m

Following this adjustment, coherent reflection events can be clearly identified at two-way travel times between 0.05 and 0.1 s, indicating improved separation between surface-wave noise and primary reflections.

A more substantial reduction of surface-wave energy was obtained by integrating several processing steps, namely f-k domain filtering, targeted attenuation of surface-wave noise, spiking deconvolution, and the application of a band-pass filter within the 14-82 Hz frequency interval.

The common-source gathers previously displayed in Figure 7, after undergoing this processing sequence, are illustrated in Figure 10.

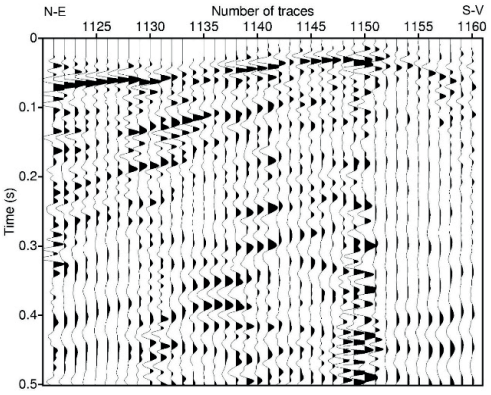



Figure 10. Common-source gather after band-pass frequency filtering applied for 14-82 Hz; shot point location at x = 30 m

Following these procedures, the gathers reveal clearer and more coherent reflection events associated with subsurface boundaries exhibiting pronounced acoustic impedance contrasts. The enhancement of reflector continuity and amplitude demonstrates the effectiveness of the combined filtering and deconvolution workflow in improving data quality. Following the spectral analysis that identified the optimal frequency content for preserving reflections, seismograms filtered within the 14-82 Hz range are advanced to the subsequent processing phase. During this stage, the data traces are reorganized by being sorted into Common Depth Point (CDP) gathers to facilitate high-resolution subsurface imaging.

Constant-velocity stacking was applied as part of the velocity evaluation procedure. For each CDP gather, traces were summed using an individual fixed velocity, producing time-domain seismic sections. Seven separate sections were generated using the following velocity values: 700 m/s, 900 m/s, 1100 m/s, 1300 m/s, 1500 m/s, 1700 m/s, and 1900 m/s. Figure 11 illustrates a seismic section that was obtained with a stacking velocity of 1300 m/s, indicated in the upper-left corner of the panel.

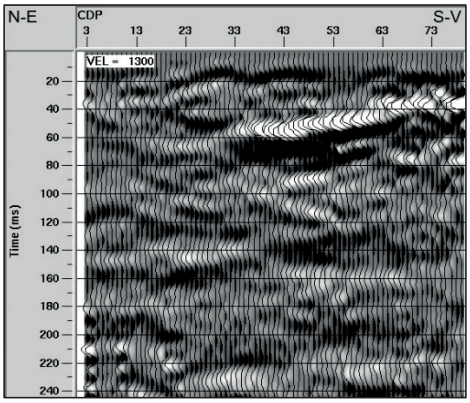



Figure 11. Section constructed for a velocity of 1300 m/s

The shallow layers, down to a few tens of meters, are most clearly delineated due to reflections in the initial sections, constructed for velocity values of 700 and 900 m/s. The reflections indicating the $CO_2$-saturated water layer are best observed in sections whose velocity values are 1100 and 1300 m/s. The sections corresponding to velocities of 1500, 1700, and 1900 m/s begin to lose quality, making the construction of further sections with increasingly higher velocity values impractical.

Depth estimation uncertainties primarily arise from inaccuracies associated with the velocity analysis. Distinct reflections can be observed at several tested velocity values. The final velocity model was established by choosing the time–velocity pairs corresponding to the CDP locations where the reflected signal exhibits maximum amplitude. Figure 12 represents the final velocity model.

A final amplitude analysis was performed on traces 40, 50, 60, and 70 (marked in red), corresponding to the final seismic time section; these traces intersect the strongest reflections associated with the water-saturated layer containing $CO_2$ (Figure 13).

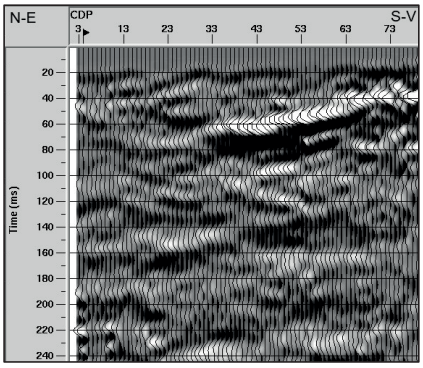



Figure 12. Final velocity model

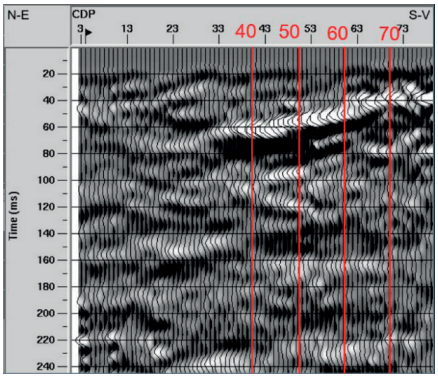



Figure 13. The final seismic section, with the analysed traces marked in red

A graph of amplitude values as a function of frequency was created for all four analysed traces (Figure 14).

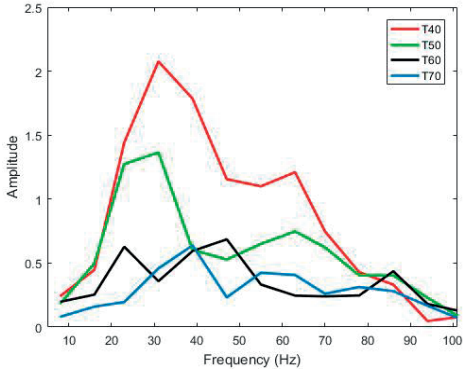



Figure 14. Amplitude spectrum for trace no. 40, 50, 60, 70

The amplitude analysis from Figure 15 shows that traces 40 and 50 exhibit the highest amplitudes, characteristic of the central part of the profile; these amplitudes reach a maximum at a frequency of 30 Hz, and they decrease as the frequency increases. In the case of traces 60 and 70, the amplitudes are slightly lower, with their maximum values also reaching 30 Hz; these values are characteristic of the final part of the profile, and similarly to the previous traces, the amplitudes decrease with increasing frequency. Additionally, traces 60 and 70 show a much smaller amplitude variation compared to traces 40 and 50.

After all these steps, the final seismic section in the time domain was converted into the depth domain for a better visualization of the geological structure intersected by the seismic profile (Figure 15).

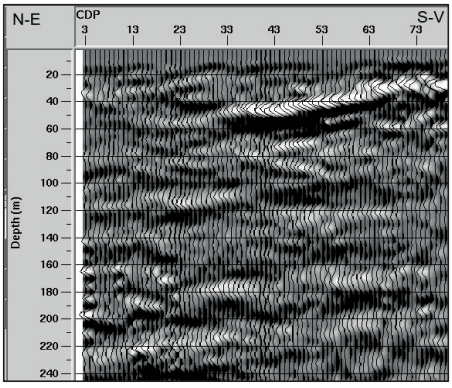



Figure 15. The final seismic section represented in the depth domain (m)

As can be observed from the final depth seismic section, the water-saturated layer containing $CO_2$ can be identified between depths of 20 and 60 m.

## CONCLUSIONS

The seismic reflection investigation carried out at Băile Lăzărești demonstrates that near-surface seismic methods can successfully image subsurface structures associated with natural $CO_2$ migration. Through a combination of elevation corrections, frequency filtering, velocity analysis, and stacking, the processing workflow significantly improved the clarity of reflection events and allowed the identification of high-amplitude reflections linked to water-saturated formations containing $CO_2$ at depths

between approximately 20 and 60 m. The results indicate that seismic data can effectively highlight the pathways through which $CO_2$-rich fluids migrate toward the surface. By providing detailed images of these natural migration routes, the study offers a valuable natural laboratory for understanding how carbon dioxide might leak in a geological storage environment. Consequently, such investigations contribute to assessing potential leakage pathways and improving the monitoring strategies required for the safe long-term storage of anthropogenic $CO_2$.

## ACKNOWLEDGEMENTS

The research leading to these results was made within the project PN 23 30 04 04 "Development of an environmental monitoring methodology for potential $CO_2$ storage sites in Romania (Dezvoltarea unei metodologii de monitorizare de mediu pentru potențialele situri de stocare de CO2 din România)", financed by the Ministry of Research, Innovation and Digitalization of Romania through the Core Program. The authors would like to acknowledge and to thank for the support of town hall of Lăzărești, who facilitated the access to the site and the smooth running of the campaign. They are also grateful to the Faculty of Geology and Geophysics, University of Bucharest, for the academic support provided during the research activities, and thank the anonymous reviewers for their valuable suggestions that helped improve the manuscript.

## REFERENCES

Annunziatellis, A., Beaubien, S. E., Bigi, S., Ciotoli, G., Coltella, M., & Lombardi, S. (2008). Gas migration along fault systems and through the vadose zone in the Latera caldera (central Italy): Implications for $CO_2$ geological storage. *International Journal of Greenhouse Gas Control, 2*(3), 353–372.

Cox, D. R., Newton, A. M. W., & Huuse, M. (2020). An introduction to seismic reflection data: Acquisition, processing and interpretation. In N. Scarselli, J. Adam, & D. Chiarella (Eds.), *Regional Geology and Tectonics: Principles of Geologic Analysis* (2nd ed., Vol. 1, pp. 571–603). Elsevier BV. https://doi.org/10.1016/B978-0-444-64134-2.00020-1

Cîndea, I. (1965). Înregistrarea și separarea undelor seismice [Recording and Separation of Seismic Waves]. In L. Constantinescu (Ed.), *Prospecțiuni Geofizice, Vol. II: metodele câmpurilor artificiale* [*Geophysical prospecting, Vol. II: Artificial field methods]* (p. 288). Technical Publishing House.

Dudu, A.-C., Pavel, A. B., Avram, C., Catianis, I., Iordache, G., Rădulescu, F., Lupașcu, N., Dragoș, A.-G., Dobre, O., & Sava, C.-Ș. (2024). Environmental assessment of the area with natural $CO_2$ emissions in Băile Lăzărești. *Scientific Papers. Series E: Land Reclamation, Earth Observation & Surveying, Environmental Engineering*, XIII.

Metz, B., Davidson, O., de Coninck, H., Loos, M., & Meyer, L. (2005). IPCC special report on carbon dioxide capture and storage. In *Intergovernmental Panel on Climate Change* (pp. 1–431). Cambridge University Press.

Pelton, J. R. (2005). Near-surface seismology: Surface-based methods. In D. K. Butler, *Near-surface geophysics* (pp. 219–250). Society of Exploration Geophysicists. https://doi.org/10.1190/1.9781560801719.ch8

Pearce, J. M., Czernichowski-Lauriol, I., Lombardi, S., Brune, S., Nador, A., Baker, J., Pauwels, H., Hatziyannis, G., Beaubien, S. E., & Faber, E. (2004). A review of natural $CO_2$ accumulations in Europe as analogues for geological sequestration. In S. J. Baines & R. H. Worden (Eds.), *Geological Storage of Carbon Dioxide* (Vol. 233, pp. 29–41). Geological Society of London. Doi: https://doi.org/10.1144/GSL.SP.2004.233.01.04

Panea, I. (2019). Shallow seismic reflection investigation of unstable sedimentary deposits in the Daneasa area, Romania. *Journal of Environmental and Engineering Geophysics*, *24*(1), 169–174. https://doi.org/10.2113/jeeg24.1.169

Sheriff, R. E., & Geldart, L. P. (1995). *Exploration seismology.* 2nd ed., pp. 47–49. Cambridge University Press.

Telford, W. M., Geldart, L. P., & Sheriff, R. E. (1990). *Applied geophysics.* 2nd ed., pp. 248–250. Cambridge University Press. https://doi.org/10.1017/CBO9781139167932

Yilmaz, Ö. (2001). Migration. In *Seismic data analysis: Processing, inversion and interpretation of seismic data,* 2nd, p. 463. Society of Exploration Geophysicists. https://doi.org/10.1190/1.9781560801580